Vol 461|22 October 2009|doi:10.1038/nature08442

ARTICLES

# SSB protein diffusion on single-stranded DNA stimulates RecA filament formation

Rahul Roy[1,2]†, Alexander G. Kozlov[3], Timothy M. Lohman[3] & Taekjip Ha[1,2,4]

**Single-stranded DNA generated in the cell during DNA metabolism is stabilized and protected by binding of ssDNA-binding (SSB) proteins. *Escherichia coli* SSB, a representative homotetrameric SSB, binds to ssDNA by wrapping the DNA using its four subunits. However, such a tightly wrapped, high-affinity protein–DNA complex still needs to be removed or repositioned quickly for unhindered action of other proteins. Here we show, using single-molecule two- and three-colour fluorescence resonance energy transfer, that tetrameric SSB can spontaneously migrate along ssDNA. Diffusional migration of SSB helps in the local displacement of SSB by an elongating RecA filament. SSB diffusion also melts short DNA hairpins transiently and stimulates RecA filament elongation on DNA with secondary structure. This observation of diffusional movement of a protein on ssDNA introduces a new model for how an SSB protein can be redistributed, while remaining tightly bound to ssDNA during recombination and repair processes.**

The primary activity of SSB proteins in DNA metabolism is to bind preferentially to ssDNA with high affinity independently of sequence[1]. However, SSB proteins also have a crucial role by interacting with a large number of proteins, directing these proteins to sites of DNA replication, recombination or repair[2]. SSB proteins are often viewed as providing only inert protection for transiently formed ssDNA; however, there is increasing evidence that SSB–ssDNA complexes are highly dynamic, which can be functionally important[3–5]. The *E. coli* SSB forms a stable homotetramer and can bind ssDNA in several modes with different properties[6]. In particular, under relatively high salt conditions ($\geq$200 mM NaCl or $\geq$ 2 mM $Mg^{2+}$ or polyamines), a low cooperativity complex forms in which ~65 nucleotides of ssDNA wrap around the tetramer ($(SSB)_{65}$ mode), interacting with all four subunits in such a way that the two ends of the ssDNA exit the protein in close proximity (referred to here as 'closed' wrapping)[6,7].

Owing to its transient role in replication, recombination and repair processes, SSB must be recycled (dissociate and reassociate with ssDNA) as well as repositioned within its ssDNA complexes. However, because *E. coli* SSB binds with extremely high affinity to ssDNA making several binding interactions[6], it remains unclear how SSB is displaced rapidly by other proteins, for example DNA polymerase or RecA, for subsequent DNA processing. Here, we demonstrate that an *E. coli* SSB tetramer can migrate via a random walk along ssDNA, thus providing a mechanism by which it can be repositioned along ssDNA while remaining tightly bound.

## Diffusional migration of SSB on ssDNA

To investigate potential movements of SSB on ssDNA, we used single-molecule fluorescence resonance energy transfer (smFRET)[8,9]. FRET efficiencies *E* from individual immobilized partial duplex DNA with a 3′ $(dT)_n$ tail ($64 \leq n \leq 131$) bound to SSB were acquired using total internal reflection fluorescence microscopy[9]. Surface immobilization and fluorescent labelling have no measurable effect on the dynamics of SSB binding mode transitions[5]. Owing to the closed wrapping in the $(SSB)_{65}$ binding mode favoured under our conditions (500 mM NaCl or 10 mM $Mg^{2+}$)[7], when SSB is bound to ssDNA of 65–70 nucleotides with its two ends labelled with donor (Cy3) and acceptor (Cy5) fluorophores, singular high FRET distributions were observed[5]. However, when a $(dT)_{69}$ tail is further extended by an additional 12 nucleotides of sequence complementary to the overhanging cohesive end of l-strand of λ-phage DNA, individual SSB–ssDNA complexes display large FRET fluctuations in the millisecond timescale (Fig. 1a). These

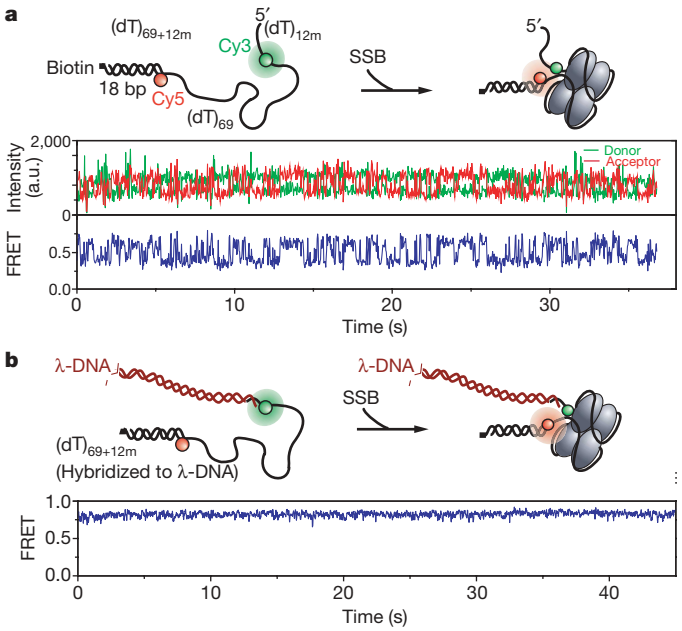


**Figure 1 | FRET fluctuations arising from diffusional migration of SSB on ssDNA. a**, With the 12-nucleotide extension to the $(dT)_{69}$ separating the donor and acceptor fluorophores, rapid fluctuations between several FRET states are observed due to diffusion of SSB on the ssDNA. a.u., arbitrary units. **b**, When the 12-nucleotide extension is hybridized to a complementary sequence, only steady high FRET values are observed.

[1]Center for Biophysics and Computational Biology, [2]Department of Physics and Center for the Physics of Living Cells, University of Illinois, Urbana-Champaign, Illinois 61801, USA. [3]Department of Biochemistry and Molecular Biophysics, Washington University School of Medicine, St Louis, Missouri 63110, USA. [4]Howard Hughes Medical Institute, Urbana, Illinois 61801, USA. †Present address: Department of Chemistry and Chemical Biology, Harvard University, Cambridge, Massachusetts 02138, USA.

fluctuations were markedly suppressed when the 12-nucleotide extension is hybridized to a cohesive end of a λ-DNA (Fig. 1b). To exclude binding and dissociation of additional SSB molecules as the cause of fluctuations, unbound SSB was removed by a buffer wash before measurements. DNA unwrapping/rewrapping dynamics, occurring in tens of microseconds in high salt concentration[3,4], is completely averaged out within our 10–30-ms time resolution[5]. We also ruled out local melting of the duplex portion as a source of fluctuation (Supplementary Information). Therefore, these fluctuations must arise from additional conformational states enabled by the 12-nucleotide extension.

To test whether the FRET fluctuations are caused by transient excursions of SSB to the extension, we varied the length of the extension ($(dT)_n$, $n = 0$–18) while keeping the ssDNA between Cy3 and Cy5 at 69 or 70 nucleotides. If an SSB tetramer binds randomly and remains fixed at the initial site of binding undergoing only transient interactions with ssDNA outside the binding site, each complex will generate a FRET distribution that is unique to the initial site of binding. However, all complexes for each construct displayed similar FRET time trajectories (Supplementary Fig. 1). Furthermore, if SSB migrates along the DNA, larger excursions away from the high FRET state are expected for longer extensions. Indeed, average FRET values decreased for longer extensions while the high FRET state was still transiently visited (Supplementary Fig. 1). The FRET distribution and the timescale of fluctuations are relatively independent of the salt concentration (Supplementary Fig. 2), presenting evidence against these FRET changes arising from binding mode transitions that display a strong salt dependence[10–12]. Hence, these fluctuations probably reflect SSB's diffusional migration on ssDNA with the different FRET values corresponding to different SSB locations.

To make unbiased assignments of FRET states, we used a hidden Markov model (HMM)-based statistical approach that determines the most likely time sequence of FRET states (Fig. 2a)[13,14]. The result is further reduced to a transition density plot[13,14] that allows the number of distinct FRET states, their FRET values and the transition rates to be estimated (Fig. 2b). We analysed SSB migration on DNA molecules with several 3′ dT tail lengths (0–12 nucleotide extension beyond 65 nucleotide binding site size) at 13 °C to slow down migration (Fig. 2a, b). Longer extensions gave several indistinguishable low FRET states in the transition density plot (Supplementary Fig. 3). For $(dT)_{69+8}$ (12 nucleotide extension from the 65 nucleotide binding site size with 69 nucleotide separation between fluorophores), six distinct FRET states were resolved (Fig. 2b) with transitions occurring between nearest neighbours. We assigned the highest FRET value ($E \approx 0.8$) to the state with SSB closest to the single-stranded–double-stranded DNA junction and lower FRET values for positions away from the junction. The rates of transition, or the 'stepping rates', were independent of the beginning and ending state of transition (Supplementary Fig. 4) and ranged between 3.0 and 4.5 $s^{-1}$ (Fig. 2c). Similar analysis yielded 5, 3 and 2 states for DNA with 8-, 2- and 0-nucleotide extensions, respectively (Supplementary Fig. 3). Therefore, every 2–4 nucleotides of DNA extension provides an additional configuration, yielding an apparent step size of about 3 nucleotides.

Because FRET fluctuations became too fast for HMM analysis above 13 °C, we used autocorrelation analysis of FRET efficiency $E$ for the temperature dependence studies (Fig. 2d). The averaged autocorrelation function plots of the SSB-$(dT)_{69+8}$ complexes were best fit by bi-exponential decays. The shorter lifetime was equal to the time resolution independent of temperature and is ascribed to photophysical or detection noise. The longer lifetime, $\tau_{long}$, displayed a monotonic temperature dependence and was attributed to SSB diffusion. The Arrhenius fit of $\ln(1/\tau_{long})$ against $1/T$ (Fig. 2e) gave an apparent activation energy of $81 \pm 7$ kJ $mol^{-1}$. Combined with the stepping rate of $\sim 4\ s^{-1}$ at 13 °C, we can then estimate a stepping rate of $\sim 60\ s^{-1}$ at 37 °C. Assuming a 3-nucleotide step size, the diffusion coefficient of an SSB tetramer along ssDNA at 37 °C is estimated to be 270 $(nucleotides)^2\ s^{-1}$.

As a further test of SSB migration on the ssDNA, we used single-molecule three-colour FRET[9,15] using a donor-labelled SSB mutant (A122C labelled with ~one Alexa555 per SSB tetramer) and two different acceptors, Cy5 and Cy5.5, attached to the two ends of a $(dT)_{130}$ (Fig. 3a). The large separation between the two acceptors eliminates any significant FRET between them. If a single SSB tetramer diffuses on the long ssDNA, high FRET events to either acceptor will be mutually exclusive. Indeed, we observed rapid and anti-correlated fluctuations of apparent FRET efficiencies to the two acceptors, $E_{app,5}$ and $E_{app,5.5}$, demonstrating that SSB truly diffuses on the DNA (Fig. 3a, b). To ensure only single SSB molecules were bound on the DNA, 1 min incubation with sub-saturating concentrations of SSB (<100 pM) was followed immediately with a buffer wash and only traces displaying single donor photobleaching events were analysed. At higher SSB concentration (10 nM), much slower FRET fluctuations were observed, probably due to binding of additional SSB (Supplementary Fig. 5).

To probe how far SSB can move on a long ssDNA, we placed Cy5 and Cy5.5 on the two ends of a $(dT)_{130}$ and Cy3 in the middle (named

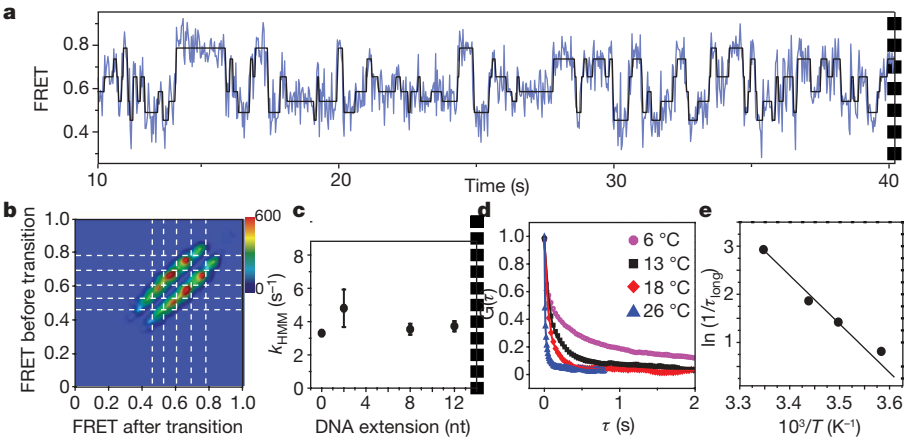


**Figure 2 | Analysis of SSB mobility on ssDNA.** **a**, Hidden Markov model (HMM)-derived idealized FRET trajectory (black) superimposed on the FRET trajectory (blue) of a single SSB-$(dT)_{69+8}$ complex. **b**, Transition density plot for $(dT)_{69+8}$ DNA. **c**, Average rates of SSB migration as a function of DNA extension length from HMM analysis. Error bars are standard error over $2(m-1)$ values of the transition rate obtained from HMM analysis where $m$ is the number of distinct FRET states ranging from 2 to 6. **d**, Autocorrelation ($G(\tau)$) analysis of FRET trajectories for $(dT)_{69+8}$ DNA fit to bi-exponential decay function for different temperatures ($T$). **e**, Arrhenius plot of apparent rates as a function of $1/T$.

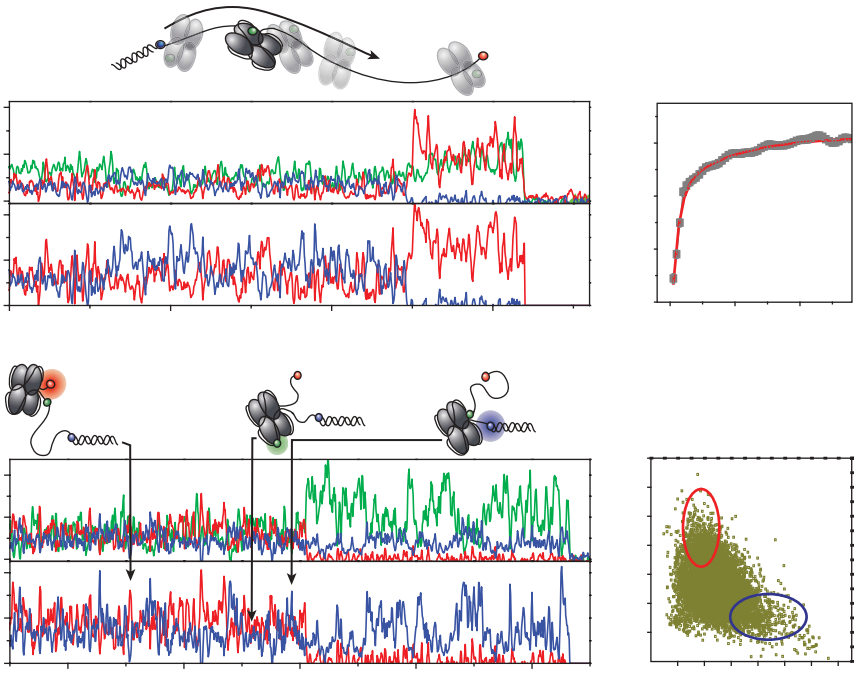

**Figure 3 | SSB diffusion on ssDNA probed with three-colour FRET. a**, Time traces of three colour intensities and the FRET efficiencies ($E_{app,5}$, $E_{app,5.5}$) display diffusion of donor-labelled SSB to acceptor-labelled ends of a $(dT)_{130}$ DNA. **b**, The average cross-correlation XC($\tau$) between $E_{app,5}$ and $E_{app,5.5}$ time traces (48 molecules) fit with a bi-exponential decay (red), demonstrating anti-correlated fluctuations. **c**, A $(dT)_{130}$ with a centrally placed donor, and acceptors at the two ends, displays excursions of unlabelled SSB to either extremity of the DNA resulting in high FRET for the corresponding acceptor. **d**, Scatter plot of $E_{app,5.5}$ against $E_{app,5}$ values (35 molecules) show mutually exclusive high FRET events (oval regions).

$(dT)_{65+65}$). This three-colour FRET scheme allows us to determine at which end the SSB was present by following the 'closed' wrapping of that DNA segment and high FRET to the corresponding acceptor (Fig. 3c). Both the dye pairs display transient high FRET states that are anti-correlated, indicating that the same SSB molecule was capable of migrating to either end of the DNA (Fig. 3c, d). Therefore, SSB can move at least 65 nucleotides via diffusion and is not constrained to its initial binding site.

## SSB displacement by RecA filament

SSB modulates the interaction between the RecA protein and ssDNA in the SOS response and recombinational repair pathway[2,16–19] and mutations in the *ssb* gene cause inefficient recombinational repair and homologous recombination[1,20–22]. A RecA filament can readily displace SSB from the DNA if assisted by RecFOR, χ-modified RecBCD or a preassembled nucleation cluster[14,23–27]. However, the mechanism of efficient SSB displacement by RecA was unclear given the tight binding of SSB to ssDNA.

Our estimated diffusion step size of SSB, ~3 nucleotides, is the same as the binding site size of a RecA monomer which is the unit of filament extension[14,28]. We therefore hypothesized that a monomer-by-monomer addition of RecA to the DNA segment freed up by SSB diffusion might convert the random walk of SSB into unidirectional movement (Supplementary Movie 1). To test this idea, we devised a three-colour FRET assay using a DNA with a 96 nucleotide 3′ tail, $(dT)_{30+65}$, labelled at positions 0, 30 and 95 with Cy5.5, Cy3 and Cy5, respectively (Fig. 4). The apparent FRET efficiencies of DNA only are low for both acceptors (~0.1), and drop to zero on RecA-ATPγS filament formation (Fig. 4a, b). SSB addition after flushing out excess RecA and ATPγS removes the RecA-ATPγS filament from the ssDNA tail, but not from the duplex DNA[14], and the ssDNA wraps around SSB, displaying higher FRET with a broad distribution that reflects SSB diffusion (Fig. 4c). The RecA-ATPγS filament remaining on the duplex serves as the nucleation cluster for filament elongation on the 3′ ssDNA tail[14] such that on addition of RecA and ATP, the elongating filament rapidly replaces SSB on the ssDNA ($E_{app} = 0$) (Fig. 4e).

Figure 4f shows the real time three-colour FRET trajectories of SSB displacement by an elongating RecA filament. Before elongation, the FRET values fluctuate rapidly due to SSB diffusion. On addition of RecA and ATP, $E_{app,5.5}$ drops first as a RecA-ATP filament initiates at the ssDNA–dsDNA junction. As this filament grows further, $E_{app,5}$ attains a steady high value. Because the Cy3 and Cy5 are separated by 65 nucleotides at the distal DNA end, we attribute this increase in $E_{app,5}$ to the repositioning of SSB to the distal end, pushed by the elongating RecA filament. Finally, complete filament elongation gives $E_{app} \approx 0$, probably accompanied by SSB dissociation. Direct excitation of the acceptors afterwards confirmed that they were not photobleached.

We used exponential fits of average FRET curves to estimate the rates of three distinct events following the addition of RecA and ATP (Fig. 4g). (1) $E_{app,5.5}$ drops from 0.3 to 0 at a rate of $k_{1,SSB} = 0.24 \pm 0.02\,s^{-1}$. We assign this to RecA filament initiation from the RecA-ATPγS nucleation site because once initiated, the decrease in $E_{app,5.5}$ is nearly instantaneous. (2) $E_{app,5}$ increases from 0.3 to 0.75 at the rate of $k_{2,SSB} = 0.2 \pm 0.01\,s^{-1}$. We assign this to RecA filament initiation and elongation by approximately ten RecA monomers on 30 nucleotides and SSB movement to the distal DNA end. The time intervals between the drop in the $E_{app,5.5}$ and the rise of $E_{app,5}$ place a lower limit of $\sim 0.6\,s^{-1}$ for the RecA elongation on a 30-mer of SSB-bound ssDNA (Supplementary Fig. 6). (3) The decrease of $E_{app,5}$ (traces synchronized when the high $E_{app,5}$ state is obtained) that we assign to SSB dissociation occurs at a much lower rate of $0.07 \pm 0.01\,s^{-1}$. The rates of filament initiation and elongation without SSB are comparable to those obtained with SSB (Fig. 4h and Supplementary Information). Furthermore, the rate of RecA elongation on bare ssDNA is about $20\,s^{-1}$ per monomer at 1 μM RecA[14] and is similar to the lower limit we determined here with SSB ($\sim 6\,s^{-1}$ per monomer), indicating that any hindrance to RecA elongation by SSB is minimal. Similar rates were observed on longer DNA where up to two SSB tetramers can bind (Supplementary Fig. 7).

Overall, the rate of SSB removal from the DNA end is approximately tenfold slower than what is expected from filament elongation alone. This observation indicates that SSB diffusion is important for

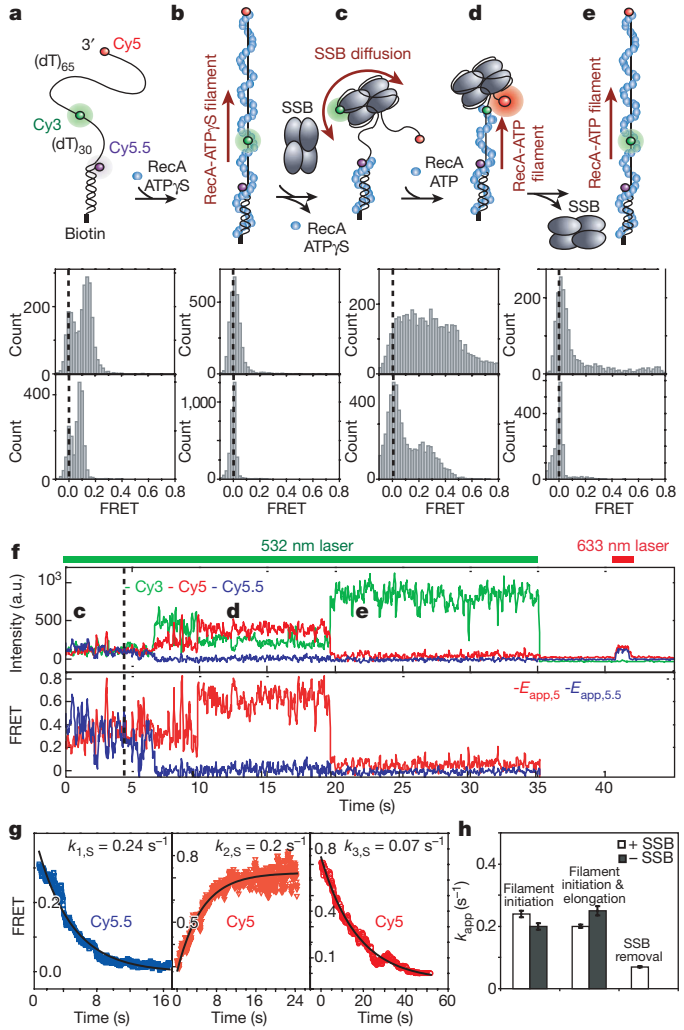


**Figure 4 | Mechanism of SSB displacement by an extending RecA filament.** **a**–**e**, Top panel, schematic of reaction steps; middle panel, $E_{app,5}$ histograms; bottom panel, $E_{app,5.5}$ histograms. **a**, DNA construct with Cy3, Cy5 and Cy5.5. **b**, RecA-ATPγS filament (5 min incubation). **c**, SSB displaces RecA filament (15 min incubation). **d**, RecA filament growth. **e**, Filament completion (2 min incubation). **f**, Three-colour FRET trajectories for segments **c**, **d** and **e**. Excitation (633 nm) at 41 s confirms active acceptors. **g**, Sub-reaction kinetics with exponential fits ($n = 46$ molecules). Left panel, average $E_{app,5.5}$ decay; middle panel, average $E_{app,5}$ increase; right panel, average $E_{app,5}$ decay after maximum. **h**, The rates of RecA filament initiation and elongation, and of SSB removal. Error bars are propagated standard errors from exponential fits in **g**.

RecA filament elongation on SSB-coated DNA. This is because before SSB reaches the DNA end, its diffusion is isoenergetic and therefore rapid, whereas its further diffusion at the 3′ end is energetically costly. This model of rectifying SSB diffusion by the directional growth of a RecA filament does not require any direct interaction of the two proteins[29] and hence could provide a general mechanism for displacement of SSB by proteins moving directionally on the ssDNA.

## SSB diffusion aids RecA on DNA hairpin

SSB inhibits RecA filament formation at low salt and high SSB concentrations[23,29], but stimulates RecA filament formation in high salt concentration[29], probably by disrupting DNA secondary structures[30,31]. Tetrameric SSBs can destabilize a DNA duplex possessing a single-strand tail that is shorter than the SSB binding site size[32], but no significant duplex disruption was observed for a tail length equal to or greater than the binding site size (Fig. 1b and Supplementary Information). We therefore investigated whether SSB can disrupt a physiologically more relevant structure, that is, a hairpin flanked by two single-stranded regions. The melting of a hairpin with a 7-base-pair stem and 3-nucleotide loop, *hp*, (Fig. 5a) is monitored via FRET between Cy3 and Cy5 attached to the ends of the hairpin in two different constructs, $(dT)_{65+hp+3}$ and $(dT)_{6+hp+65}$. A single high FRET population for an intact hairpin is partially replaced by lower FRET populations with SSB, signifying different states of hairpin unzipping (Fig. 5b). Single-molecule trajectories showed unzipping of the hairpin (Fig. 5c) with a majority displaying two-step unzipping with rate constants of $\sim$1.1–1.5 $s^{-1}$ (Fig. 5c, d; details in Supplementary Information). Hence, a single SSB tetramer transiently disrupts DNA secondary structures as stable as a 7-base-pair stem by repositioning itself on and off the hairpin segment.

Finally, we tested whether such transient melting of a DNA hairpin by SSB promotes RecA filament formation on the hairpin. Starting from a pre-nucleated RecA-ATPγS complex, a RecA-ATP filament was formed on $(dT)_{6+hp+65}$ DNA (Fig. 5e) giving rise to a $E_{app} \approx 0$ population representing filament formation over the melted hairpin (Supplementary Information). Notably, filament formation over the hairpin occurred 40-fold faster when SSB was present, demonstrating that SSB stimulates filament elongation over ssDNA that can form stable secondary structures (Fig. 5f and Supplementary Information). Interestingly, for our second construct $(dT)_{65+hp+3}$, filament formation over the hairpin remained slow even with SSB (Fig. 5f). This dependence on hairpin position further indicates that transient hairpin disruption by SSB is necessary for efficient filament elongation for the following reason. RecA filament elongation towards the 3′ end decreases the length of ssDNA available for SSB binding, forcing it to eventually dissociate. However, SSB dissociation occurs before the filament elongates to the hairpin region of $(dT)_{65+hp+3}$ such that SSB-induced hairpin melting is reversed before filament growth over the hairpin segment (Supplementary Information).

On the basis of these results, we propose that SSB diffusion along ssDNA in the low cooperative $(SSB)_{65}$ mode, where ssDNA is populated mostly with single or two tetramers[33], stimulates RecA filament elongation by transiently removing DNA secondary structures ahead of the filament, and that filament elongation via RecA monomer addition in turn directionally biases SSB diffusion (Fig. 5g and Supplementary Movie 1). For long ssDNA bound by several SSB tetramers, directional migration of an SSB tetramer caused by RecA filament elongation may increase the local SSB concentration and promote transitions to other binding modes from which SSB dissociation may be much more rapid[3,5]. If so, the findings made here may also be relevant for the removal of several SSBs from longer ssDNA.

## Mechanism and functions of SSB diffusion

How does SSB diffuse on ssDNA? One possibility is the previously suggested rolling mechanism[4,34]. SSB rolling would occur via partial unwrapping of one end segment of ssDNA from an SSB tetramer followed by re-wrapping of the other end in its place (Supplementary Fig. 8 and Supplementary Movie 1), resulting in one-dimensional random walk of SSB on ssDNA. Although our results are consistent with the rolling model, a definitive conclusion awaits further investigations.

Our work represents the first demonstration of any protein diffusing on ssDNA. By facilitating the redistribution of a tightly bound SSB tetramer along the ssDNA without full dissociation, SSB diffusion may be used in a variety of cellular processes, for example, stabilization of specific denaturation sites on superhelical DNA[35,36] and facilitation of primase activity by positioning the SSB on G4-phage-type priming systems[37]. The C-terminal region of *E. coli* SSB interacts with a variety of DNA repair enzymes and facilitates localization of these enzymes in the vicinity of ssDNA[38,39], raising the possibility that SSB acts as a mobile platform on the ssDNA for the repair and recombination machinery. The presence of homologous SSB proteins even in metazoans suggests that a similar diffusion mechanism might operate over a wide range of species[40].

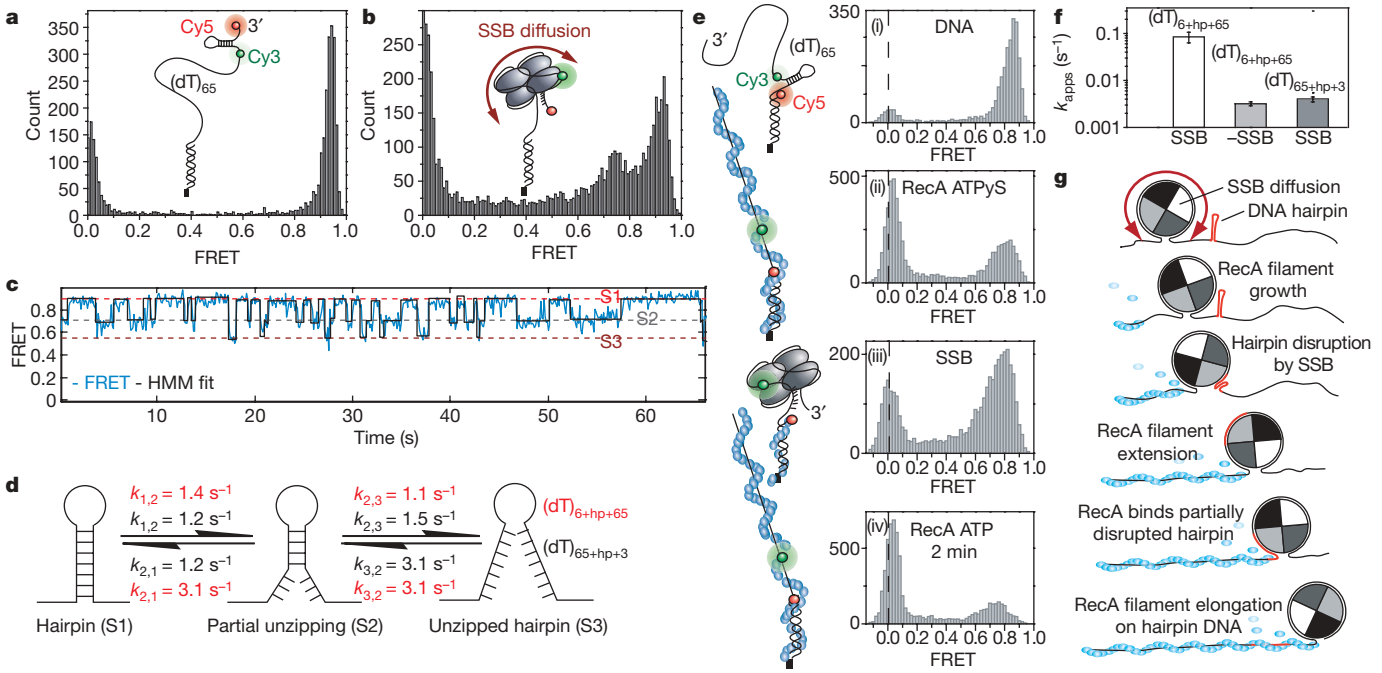


**Figure 5 | SSB diffusion promotes RecA filament growth on DNA hairpin.** **a**, FRET histograms for $(dT)_{65+hp+3}$. **b**, Hairpin destabilization by SSB induces lower FRET states. **c**, FRET trajectory of $(dT)_{65+hp+3}$ shows fluctuations between states S1 (intact hairpin), and S2 and S3 (unzipped hairpin states); HMM-derived idealized trajectory (black). **d**, Transition rates between S1, S2 and S3 for $(dT)_{65+hp+3}$ and $(dT)_{6+hp+65}$. **e**, SSB-assisted RecA filament formation on hairpin DNA. (i) Intact hairpin; (ii) RecA-ATPγS filament formation on a majority of DNA; (iii) SSB replaces the RecA-ATPγS filament restoring high FRET; (iv) RecA and ATP removes the hairpin structure. **f**, Rates of hairpin removal by extending RecA-ATP filament against hairpin position. Error bars are standard errors propagated from exponential fits (Supplementary Information). **g**, Model of SSB-assisted RecA filament growth on hairpin DNA.

## METHODS SUMMARY

Partial duplex DNA (18 base pairs dsDNA) with 3′ $(dT)_n$ tails ($n$ ranging from 64 to 131 nucleotides) carrying one donor (Cy3) and up to two acceptors (Cy5 for two-colour FRET, Cy5 and Cy5.5 for three-colour FRET) were immobilized at the duplex end on a polyethylene glycol-coated surface using biotin-neutravidin and incubated with 100 pM–1 nM SSB in imaging buffer for 1 min before flushing. Single-molecule data were acquired using wide-field total-internal-reflection (TIR) fluorescence microscopy[9] with 8–100 ms time resolution. All single-molecule measurements were performed at 23 ± 1 °C unless specified otherwise in imaging buffer (10 mM Tris (pH 8.0), 500 mM NaCl, 0.1 mM $Na_3EDTA$, 0.1 mg ml$^{-1}$ BSA) with oxygen scavenging system (0.5% w/v glucose, 1.5 mM Trolox[41] or 1% β-mercaptoethanol, 165 U ml$^{-1}$ glucose oxidase and 2,170 U ml$^{-1}$ catalase). RecA-SSB experiments were conducted in 1 μM RecA (or 10 nM SSB), 1 mM ATP (or 1 mM ATPγS) in 25 mM Tris acetate (pH 7.5), 50 mM sodium acetate, 10 mM magnesium acetate and 0.1 mg ml$^{-1}$ BSA in combination with the oxygen scavenging system.

**Received 19 March; accepted 20 August 2009.**
**Published online 11 October 2009.**

1. Meyer, R. R. & Laine, P. S. The single-stranded DNA-binding protein of *Escherichia coli*. *Microbiol. Rev.* **54,** 342–380 (1990).
2. Shereda, R. D., Kozlov, A. G., Lohman, T. M., Cox, M. M. & Keck, J. L. SSB as an organizer/mobilizer of genome maintenance complexes. *Crit. Rev. Biochem. Mol. Biol.* **43,** 289–318 (2008).
3. Kozlov, A. G. & Lohman, T. M. Kinetic mechanism of direct transfer of *Escherichia coli* SSB tetramers between single-stranded DNA molecules. *Biochemistry* **41,** 11611–11627 (2002).
4. Kuznetsov, S. V., Kozlov, A. G., Lohman, T. M. & Ansari, A. Microsecond dynamics of protein–DNA interactions: direct observation of the wrapping/unwrapping kinetics of single-stranded DNA around the *E. coli* SSB tetramer. *J. Mol. Biol.* **359,** 55–65 (2006).
5. Roy, R., Kozlov, A. G., Lohman, T. M. & Ha, T. Dynamic structural rearrangements between DNA binding modes of *E. coli* SSB protein. *J. Mol. Biol.* **369,** 1244–1257 (2007).
6. Lohman, T. M. & Ferrari, M. E. *Escherichia coli* single-stranded DNA-binding protein: multiple DNA-binding modes and cooperativities. *Annu. Rev. Biochem.* **63,** 527–570 (1994).
7. Raghunathan, S., Kozlov, A. G., Lohman, T. M. & Waksman, G. Structure of the DNA binding domain of *E. coli* SSB bound to ssDNA. *Nature Struct. Biol.* **7,** 648–652 (2000).
8. Ha, T. *et al.* Probing the interaction between two single molecules: fluorescence resonance energy transfer between a single donor and a single acceptor. *Proc. Natl Acad. Sci. USA* **93,** 6264–6268 (1996).
9. Roy, R., Hohng, S. & Ha, T. A practical guide to single-molecule FRET. *Nature Methods* **5,** 507–516 (2008).
10. Bujalowski, W. & Lohman, T. M. *Escherichia coli* single-strand binding protein forms multiple, distinct complexes with single-stranded DNA. *Biochemistry* **25,** 7799–7802 (1986).
11. Lohman, T. M. & Overman, L. B. Two binding modes in *Escherichia coli* single strand binding protein-single stranded DNA complexes. Modulation by NaCl concentration. *J. Biol. Chem.* **260,** 3594–3603 (1985).
12. Griffith, J. D., Harris, L. D. & Register, J. III. Visualization of SSB-ssDNA complexes active in the assembly of stable RecA-DNA filaments. *Cold Spring Harb. Symp. Quant. Biol.* **49,** 553–559 (1984).
13. McKinney, S. A., Joo, C. & Ha, T. Analysis of single-molecule FRET trajectories using hidden Markov modeling. *Biophys. J.* **91,** 1941–1951 (2006).
14. Joo, C. *et al.* Real-time observation of RecA filament dynamics with single monomer resolution. *Cell* **126,** 515–527 (2006).
15. Hohng, S., Joo, C. & Ha, T. Single-molecule three-color FRET. *Biophys. J.* **87,** 1328–1337 (2004).
16. Kowalczykowski, S. C. Initiation of genetic recombination and recombination-dependent replication. *Trends Biochem. Sci.* **25,** 156–165 (2000).
17. Kowalczykowski, S. C., Dixon, D. A., Eggleston, A. K., Lauder, S. D. & Rehrauer, W. M. Biochemistry of homologous recombination in *Escherichia coli*. *Microbiol. Rev.* **58,** 401–465 (1994).
18. Roca, A. I. & Cox, M. M. RecA protein: structure, function, and role in recombinational DNA repair. *Prog. Nucleic Acid Res. Mol. Biol.* **56,** 129–223 (1997).
19. Kuzminov, A. Recombinational repair of DNA damage in *Escherichia coli* and bacteriophage λ. *Microbiol. Mol. Biol. Rev.* **63,** 751–813 (1999).
20. Ennis, D. G., Amundsen, S. K. & Smith, G. R. Genetic functions promoting homologous recombination in *Escherichia coli*: a study of inversions in phage λ. *Genetics* **115,** 11–24 (1987).
21. Glassberg, J., Meyer, R. R. & Kornberg, A. Mutant single-strand binding protein of *Escherichia coli*: genetic and physiological characterization. *J. Bacteriol.* **140,** 14–19 (1979).
22. Golub, E. I. & Low, K. B. Indirect stimulation of genetic recombination. *Proc. Natl Acad. Sci. USA* **80,** 1401–1405 (1983).
23. Umezu, K., Chi, N. W. & Kolodner, R. D. Biochemical interaction of the *Escherichia coli* RecF, RecO, and RecR proteins with RecA protein and single-stranded DNA binding protein. *Proc. Natl Acad. Sci. USA* **90,** 3875–3879 (1993).
24. Anderson, D. G. & Kowalczykowski, S. C. The translocating RecBCD enzyme stimulates recombination by directing RecA protein onto ssDNA in a χ-regulated manner. *Cell* **90,** 77–86 (1997).

25. Bork, J. M., Cox, M. M. & Inman, R. B. The RecOR proteins modulate RecA protein function at 5′ ends of single-stranded DNA. *EMBO J.* **20,** 7313–7322 (2001).
26. Morimatsu, K. & Kowalczykowski, S. C. RecFOR proteins load RecA protein onto gapped DNA to accelerate DNA strand exchange: a universal step of recombinational repair. *Mol. Cell* **11,** 1337–1347 (2003).
27. Hobbs, M. D., Sakai, A. & Cox, M. M. SSB protein limits RecOR binding onto single-stranded DNA. *J. Biol. Chem.* **282,** 11058–11067 (2007).
28. Chen, Z., Yang, H. & Pavletich, N. P. Mechanism of homologous recombination from the RecA–ssDNA/dsDNA structures. *Nature* **453,** 489–494 (2008).
29. Kowalczykowski, S. C., Clow, J., Somani, R. & Varghese, A. Effects of the *Escherichia coli* SSB protein on the binding of *Escherichia coli* RecA protein to single-stranded DNA. Demonstration of competitive binding and the lack of a specific protein–protein interaction. *J. Mol. Biol.* **193,** 81–95 (1987).
30. Kowalczykowski, S. C. & Krupp, R. A. Effects of *Escherichia coli* SSB protein on the single-stranded DNA-dependent ATPase activity of *Escherichia coli* RecA protein. Evidence that SSB protein facilitates the binding of RecA protein to regions of secondary structure within single-stranded DNA. *J. Mol. Biol.* **193,** 97–113 (1987).
31. Muniyappa, K., Shaner, S. L., Tsang, S. S. & Radding, C. M. Mechanism of the concerted action of recA protein and helix-destabilizing proteins in homologous recombination. *Proc. Natl Acad. Sci. USA* **81,** 2757–2761 (1984).
32. Eggington, J. M., Kozlov, A. G., Cox, M. M. & Lohman, T. M. Polar destabilization of DNA duplexes with single-stranded overhangs by the *Deinococcus radiodurans* SSB protein. *Biochemistry* **45,** 14490–14502 (2006).
33. Bujalowski, W. & Lohman, T. M. Limited co-operativity in protein-nucleic acid interactions. A thermodynamic model for the interactions of *Escherichia coli* single strand binding protein with single-stranded nucleic acids in the "beaded", $(SSB)_{65}$ mode. *J. Mol. Biol.* **195,** 897–907 (1987).
34. Römer, R., Schomburg, U., Krauss, G. & Maass, G. *Escherichia coli* single-stranded DNA binding protein is mobile on DNA: proton NMR study of its interaction with oligo- and polynucleotides. *Biochemistry* **23,** 6132–6137 (1984).
35. Clendenning, J. B. & Schurr, J. M. A model for the binding of *E. coli* single-strand binding protein to supercoiled DNA. *Biophys. Chem.* **52,** 227–249 (1994).
36. Glikin, G. C., Gargiulo, G., Rena-Descalzi, L. & Worcel, A. *Escherichia coli* single-strand binding protein stabilizes specific denatured sites in superhelical DNA. *Nature* **303,** 770–774 (1983).
37. Sun, W. & Godson, G. N. Structure of the *Escherichia coli* primase/single-strand DNA-binding protein/phage G4oric complex required for primer RNA synthesis. *J. Mol. Biol.* **276,** 689–703 (1998).
38. Shereda, R. D., Bernstein, D. A. & Keck, J. L. A central role for SSB in *Escherichia coli* RecQ DNA helicase function. *J. Biol. Chem.* **282,** 19247–19258 (2007).
39. Lecointe, F. *et al.* Anticipating chromosomal replication fork arrest: SSB targets repair DNA helicases to active forks. *EMBO J.* **26,** 4239–4251 (2007).
40. Richard, D. J. *et al.* Single-stranded DNA-binding protein hSSB1 is critical for genomic stability. *Nature* **453,** 677–681 (2008).
41. Rasnik, I., McKinney, S. A. & Ha, T. Nonblinking and long-lasting single-molecule fluorescence imaging. *Nature Methods* **3,** 891–893 (2006).


**Supplementary Information** is linked to the online version of the paper at www.nature.com/nature.

**Acknowledgements** We thank C. Joo, S. A. McKinney, I. Rasnik, S. Hohng and S. Myong for experimental help and discussion; C. Murphy, M. Nahas and K. Raghunathan for discussion; T. Ho and A. Niedziela-Majka for help with DNA and protein preparation, respectively; and R. Porter for the SSB expression plasmid. T.H. is an employee of the Howard Hughes Medical Institute. These studies were supported by grants from the National Institutes of Health and the National Science Foundation.

**Author Contributions** R.R., A.G.K., T.M.L. and T.H. designed the experiments, A.G.K. prepared the wild-type SSB protein and the mutant SSB with fluorescent labels, R.R. performed the experiments and analysed the data; R.R., T.M.L. and T.H. wrote the manuscript.

**Author Information** Reprints and permissions information is available at www.nature.com/reprints. Correspondence and requests for materials should be addressed to T.H. (tjha@illinois.edu).

ERRATUM

doi:10.1038/nature08600

# SSB protein diffusion on single-stranded DNA stimulates RecA filament formation

Rahul Roy, Alexander G. Kozlov, Timothy M. Lohman & Taekjip Ha

*Nature* **461**, 1092–1097 (2009)

In this Article, Figure 3 was printed incorrectly with missing labels. The correct figure is shown below.